Available online at www.sciencedirect.com
SCIENCE DIRECT®
Synthetic Metals 150 (2005) 145–151
SYNTHETIC METALS
www.elsevier.com/locate/synmet

Thermal degradation of the dielectric relaxation of 10–90% (w/w) zeolite-conducting polypyrrole composites

A.N. Papathanassiou [a,b,*], J. Grammatikakis [a], I. Sakellis [a], S. Sakkopoulos [c], E. Vitoratos [c], E. Dalas [d]

[a] *University of Athens, Department of Physics, Section of Solid State Physics, Panepistimiopolis, GR 157 84 Zografos, Athens, Greece*
[b] *Hellenic Army Academy, Section of Applied Physics, GR 166 73 Vari, Greece*
[c] *University of Patras, Department of Physics, GR 265 00 Patras, Greece*
[d] *University of Patras, Department of Chemistry, GR 265 00 Patras, Greece*

Received 26 October 2004; received in revised form 29 January 2005; accepted 30 January 2005
Available online 16 March 2005

Abstract

The effect of thermal aging of 10–90 wt% zeolite-conducting polypyrrole composite on its dielectric properties is studied in the frequency range 10^{-2} to 2×10^6 Hz from room temperature to liquid nitrogen temperature. A dielectric relaxation mechanism, which appears in the fresh samples, is influenced by the thermal annealing. The frequency f_{max} where a maximum of a dielectric loss peak is located decays exponentially with the aging time and the intensity of the loss peaks shows a maximum at intermediate aging time. A modified Williams–Landel–Ferry law describes the temperature variation of f_{max} in all specimens. Increasing activation energy values on increasing the aging duration are obtained. The temperature dependence of f_{max} and the activation energy (regarded as the height of a potential barrier) are different from those characterizing the macroscopic conductivity, which is described by the charging energy limited tunneling model. The intensity of the dielectric mechanism in thermally treated samples deviates from the linear decrease with inverse temperature occurring in fresh polypyrrole. Although the thermal degradation of the logarithm of the dc conductivity decays proportional with the root of the aging time, the equivalent conductivity obtained from the dielectric data decays exponentially with aging duration. Time constants are obtained in both cases. The model of Barton–Nakajima–Namikawa (BNN) can hardly interconnect the dc conductivity with the relaxation process in fresh sample. The divergence augments with the aging time. The thermal aging law and the inadequacy of the BNN model probably indicates that the dc process is probably irrelevant to the relaxation process.

PACS: 72.80.Le; 77.22.Gm; 71.20.Rv

Keywords: Conducting polymers; Zeolite; Polypyrrole; Electrical conductivity; Permittivity; Thermal aging

1. Introduction

Conductivity phenomena in conducting polypyrrole are the subject of numerous theoretical and experimental works, so as to have a unified picture of charge transfer in these materials [1,2]. The applications of conducting polymers are wide such as solar cells, pH electrodes, media for hydrogen storage, electronic devices, etc. [3–5]. Polypyrrole is complexed with zeolite to produce high efficiency anodes of power cells. Zeolite contains pores, channels and cages of different dimensions and shapes and their surface is negatively charge-balanced with exchangeable cations [4]. Zeolite–polypyrrole composites have the advantage of fast electronic mobility of polypyrrole and the capability of zeolite to incorporate cations into its structure.

The study of the thermal degradation of the electrical conductivity has been used to determine the stability of conducting polymers and blends, a crucial factor for their use in practical applications. In conductive polypyrrole, which

* Corresponding author. Tel.: +32 10 722 4444; fax: +32 10 766 1707.
E-mail address: apapathan@in.gr (A.N. Papathanassiou).

0379-6779/$ – see front matter © 2005 Elsevier B.V. All rights reserved.
doi:10.1016/j.synthmet.2005.01.021

has the granular metal structure, aging is attributed to the decreasing of the conducting grain size with a kinetic resembling a corrosion mechanism [6,7,3]. Moreover, the thermal degradation law serves as a tool to check if the structure of the conducting polymer is homogeneous or heterogeneous, of the granular metal type [8]. Recently, we studied the dielectric response of conductive polypyrrole and zeolite-conductive polypyrrole at various weight fractions [9]. The behavior varies from metallic to insulating, depending on the percentage weight fraction. The 10–90% (w/w) zeolite–polypyrrole has a semi-conductive behavior with well-defined dielectric loss peak within the temperature range from liquid nitrogen temperature to room temperature. In the present work, we will see whether the dielectric loss (i.e., a bell-shaped peak in the imaginary part of the permittivity versus frequency diagram when plotted in a log–log representation) peak is sensitive to the thermal aging and if any relation with the thermal degradation of the steady current exists. To the best of our knowledge, studies on the effect of thermal annealing on the dielectric response is lacking in the literature.

2. Experimental

Freshly distilled pyrrole (Merc AR) was polymerized in the presence of $FeCl_3$ as oxidant in hydrochloric acid–water solutions at pH 2.00 in an ice bath. The molar ratio of oxidant to monomer was 1:1 and the solvent used was triply distilled water. Polypyrrole was obtained as black powder and was purified by Soxhlet extraction for 36 h [10]. Zeolite was purified according to the following procedure [11,12]. First, it was dispersed in distilled water and the emulsio was stirred for 24 h. The suspension then was purified by sedimentation to collect the <2 μm in diameter fraction, washing with 1 M CH_3COONa and CH_3COOH (pH 5) to remove carbonate. Then washing with 0.3 M sodium citrate, 1 M $NaHCO_3$ and $Na_2S_2O_4$ to remove free iron sulfide took place. The precipitate was dispersed in 100 ml 1N NaCl and was stirred for 30 min. The emulsion was repeatedly centrifuged in order to obtain the same type of exchange cations. Purified zeolite was added to the polypyrrole solutions in the proper quantity to obtain 10, 25, 35 and 50% (w/w) content of the zeolite. The precipitates were washed with 1N HCl and dried overnight under nitrogen atmosphere. From these polypyrrole/zeolite disc shaped specimens 13 mm in diameter and about 1.5 mm thick were made in a IR press.

The dielectric measurements were performed by placing the specimens in a sample holder of a vacuum cryostat operating at 1 Pa. Good contact between the surfaces of the specimen and the electrodes was achieved by attaching silver paste. The temperature was monitored from room temperature to liquid nitrogen temperature. The measurements were performed in the frequency range 10^{-2} to 2×10^6 Hz by a Solartron SI 1260 impedance analyzer. Thermal aging was taking place at atmospheric conditions inside a furnace thermostated at 70 °C.

3. Results and discussion

The real and the imaginary parts of the permittivity (ε' and ε'') are related, respectively, with the real and the imaginary parts of the complex conductivity (σ' and σ'') by the following relations [13]:

$$\varepsilon'(\omega) = \varepsilon_\infty + \frac{\sigma''(\omega)}{\varepsilon_0 \omega} \quad (1)$$

$$\varepsilon''(\omega) = \frac{\sigma'(\omega)}{\varepsilon_0 \omega} = \frac{\sigma_0}{\varepsilon_0 \omega} + \varepsilon''_d \quad (2)$$

where ε_0 is the permittivity of free space, ε_∞ the high frequency permittivity, σ_0 the dc conductivity and ε''_d is the imaginary part of the permittivity after subtracting the dc component:

$$\varepsilon''_d = \frac{\sigma'(\omega) - \sigma_0}{\varepsilon_0 \omega} \quad (3)$$

3.1. Temperature dependence of the relaxation peaks

Isotherms of the measured imaginary part of the dielectric constant versus frequency at 135 K for fresh and thermally treated sample are depicted in Fig. 1. At a given temperature,

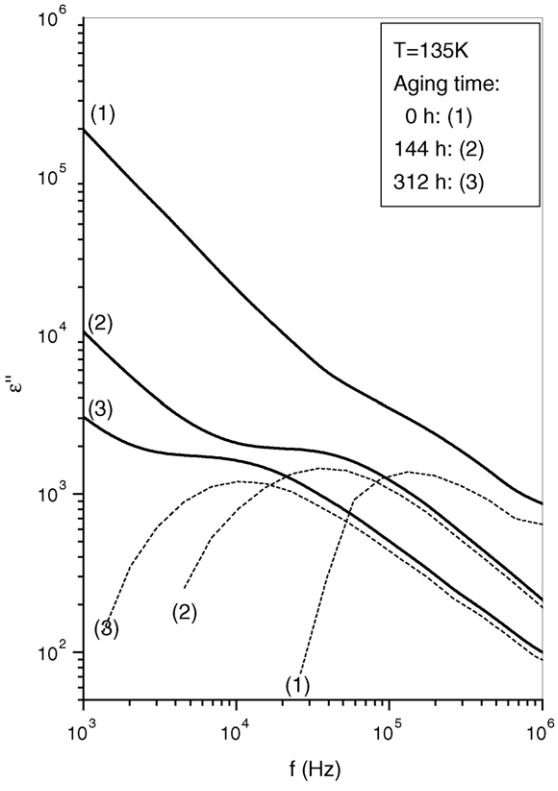

Fig. 1. The measured imaginary part of the permittivity (solid lines) vs. frequency at 135 K for the fresh and thermally aged 10–90% (w/w) zeolite–polypyrrole composite. The dashed lines are the dielectric loss peaks obtained from the measured valued of ε'' after subtracting the dc conductivity component.

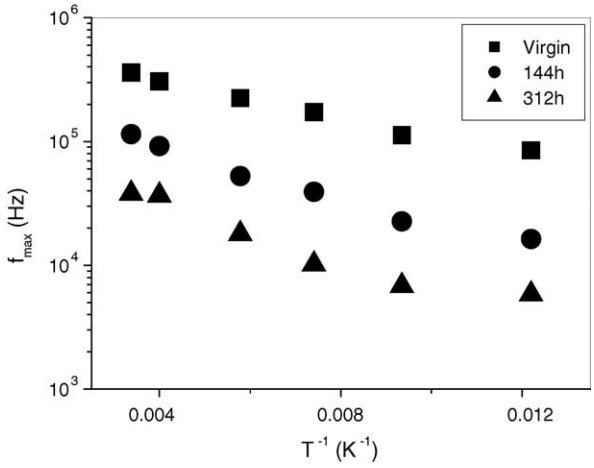

Fig. 2. The location of the dielectric loss peaks vs. reciprocal temperature for the fresh and thermally aged 10–90% (w/w) zeolite–polypyrrole composite.

$\log \varepsilon''(\log f)$ decreases linearly in the low frequency range, with slope equal to -1, indicating that the conductivity is frequency independent. Permittivity is suppressed after the thermal treatment, due to the thermal degradation of the dc conductivity. At higher frequencies, $\log \varepsilon''(\log f)$ diverges from linearity due to the presence of a dielectric relaxation mechanism. Relaxation peaks (i.e., ε''_d versus frequency) are obtained after subtracting of the masking dc component from the measured ε'' values (Fig. 1). The dc component becomes weaker on increasing the thermal aging duration as a result of the thermal degradation of the electrical conductivity. The relaxation peak shifts toward lower frequencies for increasing aging time.

In Fig. 2, the frequency f_{max} where a relaxation peak has its maximum is plotted as a function of temperature, for fresh and aged samples. The physical meaning of f_{max} is found in $f_{max}(T) = 1/2\pi\tau(T)$ [13], where τ is a characteristic relaxation time. Within this frame, thermal aging augments the relaxation time, i.e., the relaxation time increases after aging. The experimental data deviate from a simple Arrhenius law, i.e., $f_{max} = f_0 \exp(-E/kT)$, where f_0 is the constant, k the Boltzmann's constant and E is the activation energy corresponding to the relaxation process. We have used a modified Williams–Landel–Ferry (WLF) relation [14] to match the experimental results:

$$f_{max} = f_0 \exp\left(-\frac{T_1}{T + T_0}\right) \quad (4)$$

where T_1 and T_0 are fitting constants. Note that the sign of T_0 is negative for rotating permanent dipoles. $E \approx KT_1$ is labeled here as the activation energy for relaxation, to keep a common notation with the dc conductivity analysis mentioned below. E is the height of the effective potential energy barrier separating sites involved in the relaxation process. The parameters obtained by fitting of the last equation (Eq. (4)) to the experimental data appearing in Fig. 2 are enlisted in Table 1. The positive values of the parameter T_0 indicate that the nature of relaxation does not involve the rotational modes of permanent electric dipoles. The curvature observed in the $f_{max}(T)$ diagrams (Fig. 2) indicates that the phenomenological 'apparent' activation energy E_{app}, which is defined as the percentage variation of the relaxation time upon T^{-1} ($E_{app} \equiv \mathrm{d}\ln\tau(T)/\mathrm{d}(1/kT) = -\mathrm{d}\ln f_{max}(T)/\mathrm{d}(1/kT)$), increases at high temperatures. This behavior is opposite to that observed in dipolar relaxation, where cooperative phenomena reduce the apparent activation energy with increasing temperature [15].

Table 1
The parameters of the modified Williams–Landel–Ferry (WLF) model $f_{max} = f_0 \exp(-T_1/T + T_0)$ (Eq. (4)) used to fit the temperature dependence of the frequency values f_{max} where the relaxation peaks reach a maximum

Aging time (h)	f_0 (Hz)	T_1 (K)	T_0 (K)	E (eV)
0	$(8.1 \pm 0.7) \times 10^5$	272 ± 5	37 ± 1	0.0234 ± 0.0003
144	$(6.9 \pm 0.2) \times 10^5$	650 ± 20	96 ± 3	0.056 ± 0.002
312	$(2.9 \pm 0.2) \times 10^5$	770 ± 40	108 ± 6	0.066 ± 0.004

It is worth noticing how well the qualitative visualization of Fig. 2 agrees with the quantitative results obtained from the analysis of the experimental data (Table 1). The increase of the relaxation times with aging matches well with the increase of the activation energy values upon aging duration (Table 1). It seems that the reduction of the conductive grains in the polymer phase yield an increase in the effective potential barrier separating sites involved in the relaxation process. This statement is confirmed by dc conductivity and thermopower experimental data [6]. Moreover, the shrinking of the conductive grains with aging is α general feature of conducting polypyrrole, polyaniline and their blends [16,17].

The intensity of the relaxation peaks $\Delta\varepsilon = \varepsilon_s - \varepsilon_\infty$, where ε_s is the static permittivity and ε_∞ is the high-frequency one, is plotted as a function of temperature in Fig. 3. Thermal aging results in an increase of the $\Delta\varepsilon$ values compared with those of the virgin specimen, indicating that, despite the thermal degradation of the dc conductivity, more charge

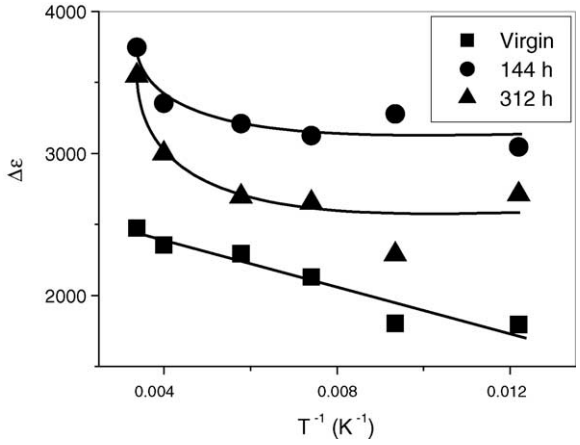

Fig. 3. The intensity of the dielectric loss peaks vs. reciprocal temperature for the fresh and thermally aged 10–90% (w/w) zeolite–polypyrrole composite.

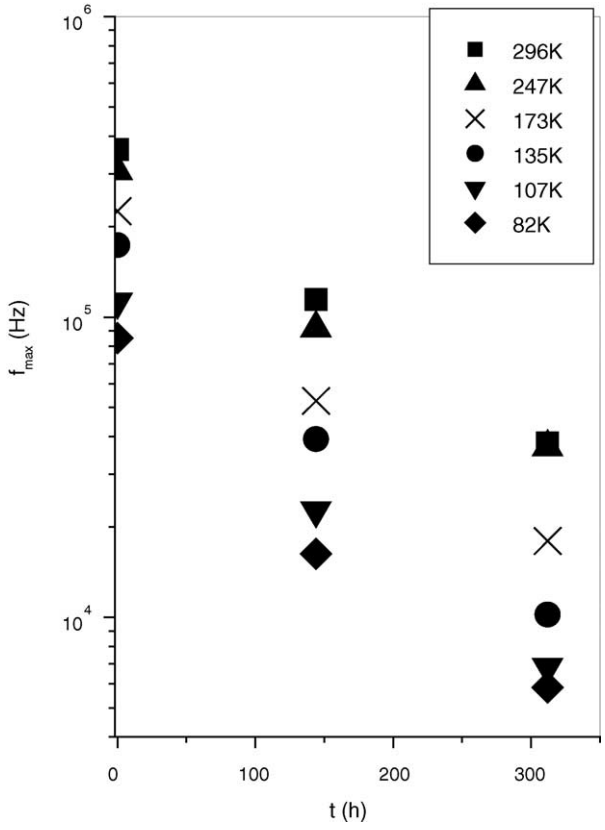

Fig. 4. Thermal degradation of the peak maximum f_{max}.

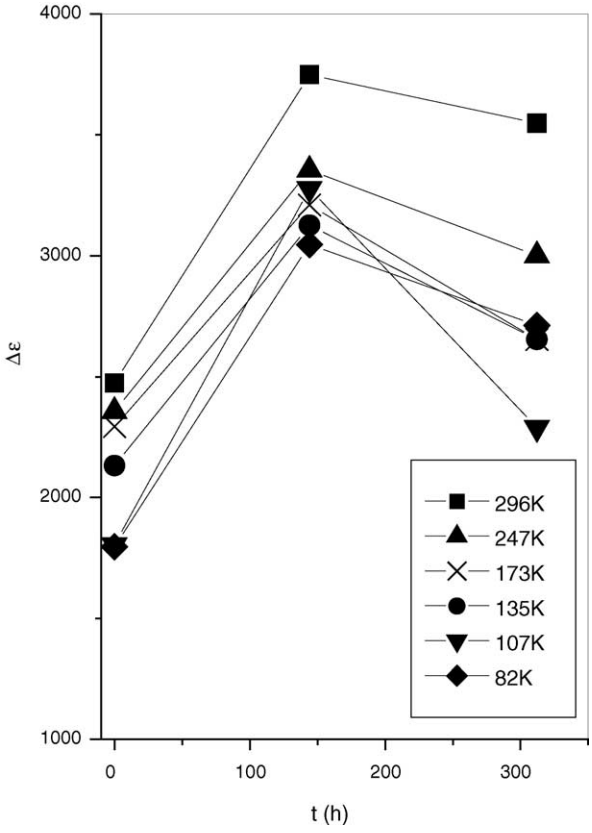

Fig. 5. Thermal degradation of the intensity of the relaxation peak. Data points are connected with straight lines for a better understanding of the diagram.

carriers contribute to the ac response after thermal aging. In the ac response the charge carriers oscillate between adjacent potential wells, though in the dc conductivity have to move a distance comparable to the sample dimensions to produce a macroscopically measurable result. With aging, the polymer chains among other distresses, suffer division in smaller pieces, which prevents carriers from long-range displacement, however, giving them the possibility to contribute to ac conductivity. $\Delta\varepsilon$ decreases with temperature as $\Delta\varepsilon \propto T^{-1}$ for fresh sample (Fig. 3). This behavior is predicted by the random free-energy barrier model [18]. A deviation from the T^{-1} law is observed in aged specimens: In the high temperature region such divergence is strong, while $\Delta\varepsilon$ seems to stabilize below 200 K. The peaks shift to lower frequencies on increasing aging time as can be seen in Fig. 4, where f_{max} decreases monotonically with aging. The dielectric intensity exhibits a maximum at about 144 h annealing (Fig. 5).

The low frequency region of the permittivity spectra is characterized by the frequency independent conductivity σ_0. The latter is related with macroscopic conductivity, whereas charge carriers transfer along the volume of the specimen under the influence of slowly varying external electric field. The temperature variation of the dc conductivity of polypyrrole is usually governed by the fluctuation-induced tunneling (FIT) model, in which parabolic insulating barriers internee between large conducting grains [19,20]. In FIT model the conductivity is given by:

$$\sigma_0(T) = C \exp\left(-\frac{T_{1\sigma}}{T + T_0}\right) \quad (5)$$

This relation was used to analyze $\sigma_0(T)$ of fresh polypyrrole and zeolite polypyrrole composites with 10, 25 and 35 wt% in zeolite [9]. The fit was satisfactory except for the 10 wt% composite, where the fit was poor, i.e., $C = (6 \pm 9) \times 10^{-3}$ S/cm, $T_{1\sigma} = (2000 \pm 2000)$ K and $T_0 = (300 \pm 200)$ K [9]. Things are worse for the thermally treated 10–90% (w/w) zeolite polypyrrole blend, as Eq. (5) fails at all to match the $\sigma_0(T)$ data points. Alternatively, in the temperature range where our experiments were carried out, the dc conductivity of polypyrrole might well be described by the charging energy limited tunneling (CELT) model [21,22] that is consistent with the picture of a material with heterogeneous structure of the granular metal type:

$$\sigma_0(T) = C \exp\left(-\left(\frac{T_{1\sigma}}{T}\right)^{1/2}\right) \quad (6)$$

where C is a pre-exponential factor and $T_{1\sigma}$ is a constant which, when multiplied by the Boltzmann's constant, results in the activation energy of the dc conductivity (i.e., $E = kT_{1\sigma}$). Note that such equation applies in low conductivity samples

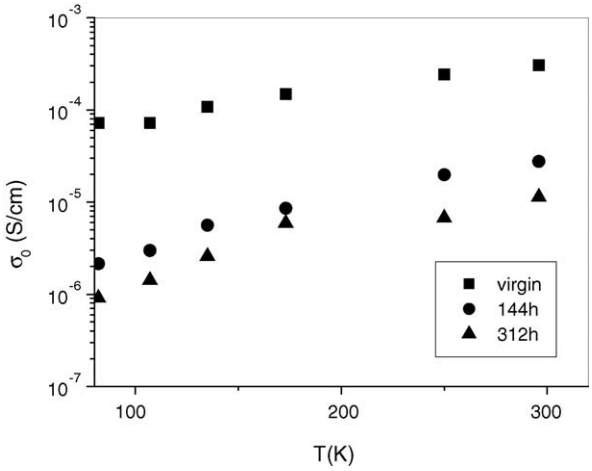

Fig. 6. Temperature independent conductivity σ_0, which corresponds to the macroscopic conductivity, vs. temperature.

of polypyrrole [23–26]. Eq. (6) is typical for quasi-1D hopping [27] (probably hopping between localized states along a polymeric chain that interconnects two crystalline (metallic) regions) or 3D hopping in the presence of electron–electron interactions or tunneling between mesoscopic metallic islands [28]. The CELT model describes well the $\sigma_0(T)$ data depicted in Fig. 6. The parameters of Eq. (6) that best fit the data points are enlisted in Table 2. The increase of the activation energy after the thermal annealing could be attributed to the reduction of the size of conducting grains, but the maximum observed at 144 h contradicts this idea.

Comparing Eq. (4) with Eq. (6), we note that f_{max} and σ_0 have different temperature dependencies. Additionally, the activation energy values for relaxation (Table 1) are an order of magnitude smaller than those corresponding to the dc transport (Table 2). Macroscopic conductivity traces the higher potential energy barriers, while relaxation involves hopping between adjacent sites separated by lower barrier. Moreover, the activation energy for relaxation increases with aging time, while, for the dc process, it maximizes at 144 h duration. The temperature-dependence results indicate that the short-range backward–forward hopping involves a different process from than that of the macroscopic conductivity.

3.2. Thermal degradation of the electrical conductivity and the dielectric response

The concept of thermal degradation of the dc conductivity σ_{dc} of conductive polymers on aging duration has attracted the interest of many researchers. The experimental data usually obey the following law [7,8]:

$$\sigma_{dc}(t) = \sigma_{dc}(t=0)\exp\left(-\sqrt{\frac{t}{\tau_1^{aging}}}\right) \quad (7)$$

where t denotes the aging time, $\sigma_{dc}(t=0)$ is the dc conductivity of the fresh specimen and τ_1^{aging} is a time constant; the larger τ_1^{aging} is, the more stable the material is. dc conductivity values were obtained from the low-frequency domain of our measurements, where conductivity is frequency independent and is labeled σ_0 and corresponds to macroscopic charge flow along the whole volume of the specimen. In Fig. 7, the logarithm of σ_0 is plotted as a function of $t^{1/2}$. The phenomenon is well described by the above mentioned degradation law (Eq. (7)). The aging time constant τ_1^{aging} obtained by applying Eq. (7), at various temperatures, varies from 82 h (at $T = 82$ K) to 150 h (at room temperature).

To compare the thermal degradation of the short-range conductivity (i.e., the localized ac conductivity backward–forward motion of charge carriers) with the long-range one (i.e., σ_0), it is necessary to calculate the equivalent conductivity σ^* from the dielectric data [13]:

$$\sigma^* = 2\pi f_{max}\varepsilon_0\,\Delta\varepsilon \quad (8)$$

The equivalent conductivity data do not obey Eq. (7). Instead, the thermal annealing results in a simple exponential decay:

$$\sigma^*(t) = \sigma^*(t=0)\exp\left(-\frac{t}{\tau_2^{aging}}\right) \quad (9)$$

where τ_2^{aging} denotes the characteristic time constant. As can be seen in Fig. 8, Eq. (9) fits very well the experimental data. The aging time-constant τ_2^{aging} varies from 280 to 380 h. The aging time-constants τ_1^{aging} and τ_2^{aging} at various temperatures

Table 2
Parameters of the charging energy limited tunneling model (CELT) obtained by fitting Eq. (6) to the $\sigma_0(T)$ data, which are determined from the frequency-independent conductivity (low frequency region)

Aging time (h)	C (S/cm)	$T_{1\sigma}$ (K)	E (eV)
0	$(2.3 \pm 0.5) \times 10^{-3}$	1200 ± 200	0.10 ± 0.01
144	$(9 \pm 2) \times 10^{-4}$	3600 ± 400	0.31 ± 0.04
312	$(1.6 \pm 0.9) \times 10^{-4}$	2200 ± 900	0.19 ± 0.08

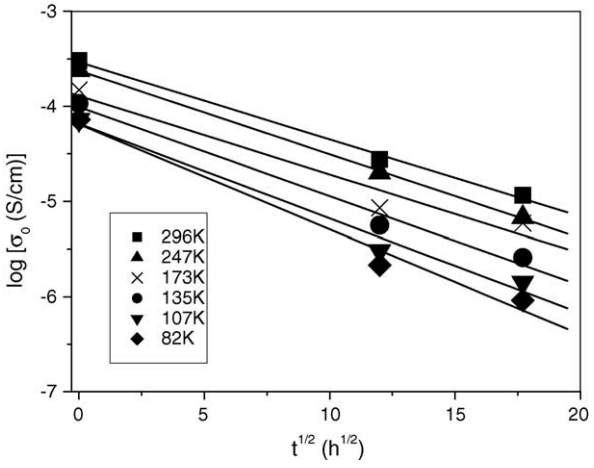

Fig. 7. The logarithm of the dc conductivity component σ_0 vs. the square root of the aging time. Lines are the best fits to the data points.

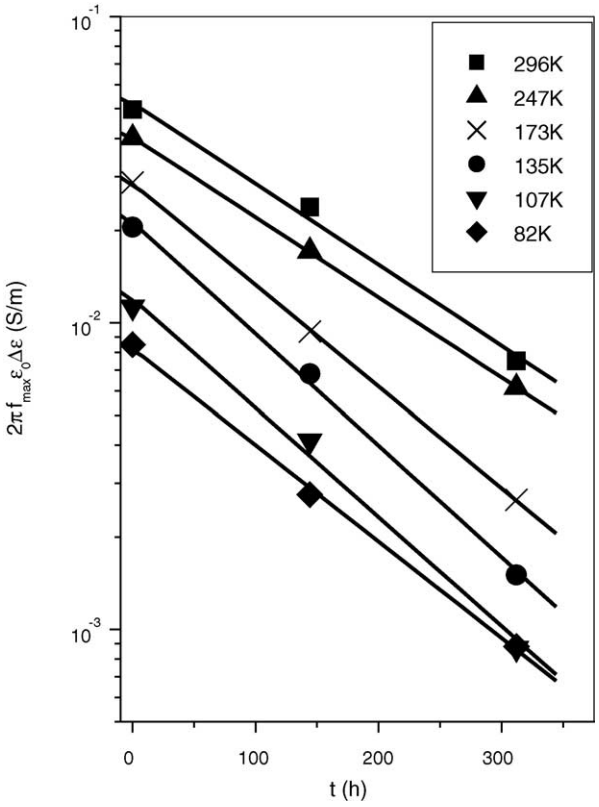

Fig. 8. The quantity $2\pi f_{max}\varepsilon_0\,\Delta\varepsilon$ vs. aging time. Lines are the best fits to the data points.

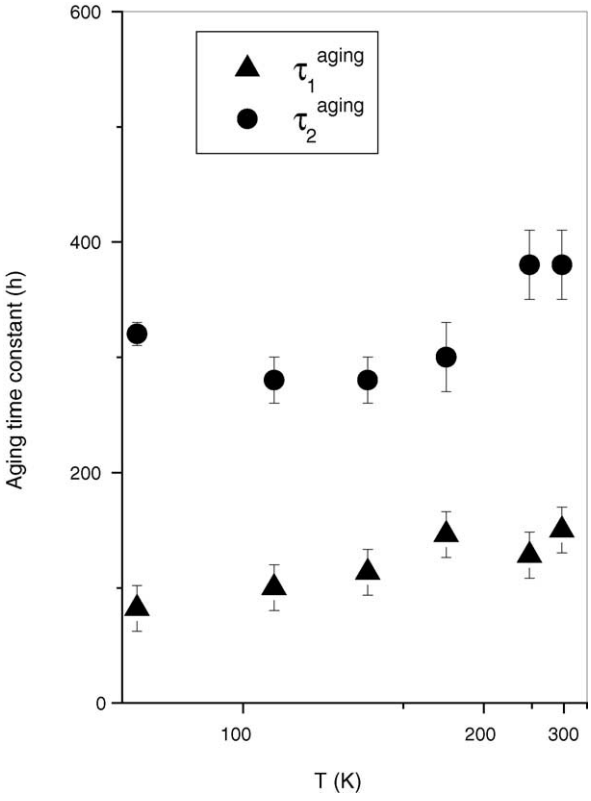

Fig. 9. Time constants of the thermal degradation of the dc component of the conductivity (τ_1^{aging}) and dielectric relaxation peak (τ_2^{aging}).

are depicted in Fig. 9. An increase of the time constant with temperature is a common trend in this diagram. It is worth to notice that the largest time constant values obtained from the degradation of the dielectric loss peak are observed above 200 K and it is perhaps related with the increased values of $\Delta\varepsilon$ detected in the same region (Fig. 3). The different manner in which σ_0 and $2\pi f_{max}\varepsilon_0\,\Delta\varepsilon$ degrade with the thermal treatment duration indicates that long-range and short-range electric charge transport involve different processes.

3.3. *Effect of thermal aging on the applicability of the Barton–Nakajima–Namikawa model*

dc and ac conductivity are interconnected through the Barton–Nakajima–Namikawa model [29–31]. The position of the relaxation mechanism be determined by the dc conductivity, through the so-called BNN condition:

$$f_{max,BNN} = \frac{1}{2\pi p}\frac{\sigma_0}{\varepsilon_0\,\Delta\varepsilon} \tag{10}$$

where p is a constant of the order of unity. Such correlation in conductive polymers [15,32,33,9] is justified in some cases but fails in others. In Fig. 10, $2\pi f_{max}\varepsilon_0\,\Delta\varepsilon$ is plotted against σ_0. We observe that the experimental data points can hardly match the prediction of the BNN model for the fresh sample, but, as the aging time augments, the divergence increases. Such disagreement, that was observed in some amorphous materials, was attributed to over-simplifications of the theoretical model: the material characteristics and the nature of charge carriers are ignored, a fixed hopping mechanism is assumed, dipole relaxation and many body long-range interaction are ignored, etc. [15]. It seems that the validity of the BNN model depends strongly on the concentration of charge carriers, i.e., the degree of protonation of the polymeric phase. Coupling between dc conductivity and dielectric

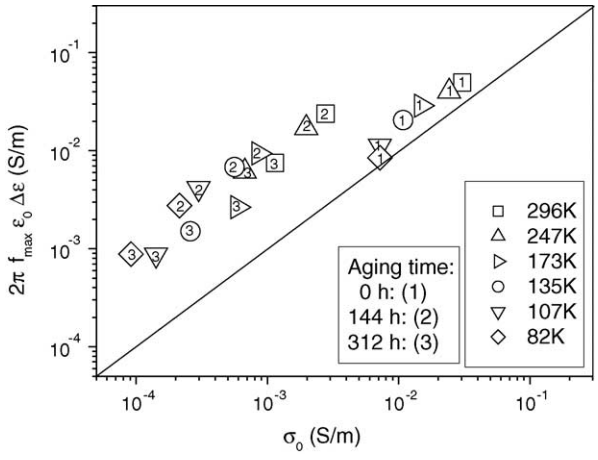

Fig. 10. Log–log representation of $2\pi f_{max}\varepsilon_0\,\Delta\varepsilon$ vs. σ_0 for fresh and aged specimens. The solid line represents the prediction of the BNN model.

response might exist provided that the density of polarons is high. We believe that this might be a reason that the BNN model is partially successful in conducting polymers and composites.

4. Conclusion

The dielectric response of the 10–90% (w/w) zeolite-conductive polypyrrole composite is sensitive to the thermal aging duration. Zeolite has a cavity structure, in which pores, channels and cages of different dimensions and shapes are included, providing an extended polymer–zeolite surface of contact and protecting conducting polymer from the air, slowing down its aging rate. Polarons hopping within the polymer and ionic conduction through the zeolite are coupled to the macroscopic conductivity. The electric properties of the blend resemble those of conducting polypyrrole, indicating that electronic transfer practically dominates. Thermal annealing induces changes in the activation energy and the intensity of the relaxation mechanism. The temperature variation of the position of the relaxation peak follows different law than the macroscopic conductivity does. The activation energy values for relaxation are an order of magnitude smaller than those obtained from the frequency-independent conductivity. The dc component of the conductivity versus aging time follows different law from that of the ac response. The validity of BNN model gradually becomes poor on increasing aging time. These combined results indicate that the long-range charge transfer (corresponding to the dc conduction) and short-range hopping (corresponding to the ac relaxation) are uncoupled. As far as we know, it is the first time that thermal aging is used as a tool to monitor dielectric response in conductive polymeric systems.

Acknowledgements

The present research was financed from the Operational Program for Education and Initial Vocational Training ‘EPEAEK-2’ within the frame of project “Pythagoras: Support of University Research Groups” by 75% from EU Fund and 25% from National Resources.

References

[1] K. Lee, A.J. Heeger, Phys. Rev. B 68 (2003) 035201.
[2] V.N. Prigodin, A.J. Epstein, Synth. Met. 125 (2002) 43.
[3] E. Dalas, S. Sakkopoulos, E. Vitoratos, Synth. Met. 114 (2000) 365.
[4] M. Nakayama, J. Yano, K. Nakaoka, K. Ogura, Synth. Met. 138 (2003) 419.
[5] J. Weitkamp, M. Fritz, S. Eritz, Int. J. Hydrogen Energy 20 (1995) 967.
[6] B. Sixou, N. Mermilliod, J.P. Travers, Phys. Rev. B 53 (1996) 4509.
[7] S. Sakkopoulos, E. Vitoratos, E. Dalas, Synth. Met. 92 (1998) 63.
[8] T.L. Tansley, D.S. Maddison, J. Appl. Phys. 69 (1991) 7711–7713.
[9] A.N. Papathanassiou, J. Grammatikakis, I. Sakellis, S. Sakkopoulos, E. Vitoratos, E. Dalas, J. Appl. Phys. 96 (2004) 3883.
[10] C. Menardo, M. Nechtschein, A. Rousseau, J.P. Travers, Synth. Met. 25 (1988) 311.
[11] R.D. King, D.C. Nocera, T.J. Pinnavaia, J. Electroanal. Chem. 236 (1987) 43.
[12] K.G. Fournaris, M.A. Karakasides, K. Yiannakopoulou, D. Petridis, Chem. Mater. 11 (1999) 2372.
[13] P. Debye, Polar Molecules, Dover Publications, New York, 1945.
[14] M.L. Williams, R.F. Landel, J.D. Ferry, J. Am. Chem. Soc. 77 (1955) 3701.
[15] S. Capaccioli, M. Luccher, G. Ruggeri, J. Phys. Condens. Mater 19 (1998) 5595.
[16] E. Dalas, E. Vitoratos, S. Sakkopoulos, P. Ma1lkaj, J. Power Sources 128 (2004) 319.
[17] E. Vitoratos, Curr. Appl. Phys., in press.
[18] J.D. Dyre, J. Appl. Phys. 64 (1988) 1456.
[19] P. Sheng, Phys. Rev. B 21 (1980) 2180–2195.
[20] G. Paasch, D. Schmeisser, A. Bartl, H. Naarman, L. Dunsch, W. Gopel, Synth. Met. 66 (1994) 135–142.
[21] P. Sheng, B. Abeles, Y. Arie, Phys. Rev. Lett. 311 (1973) 44.
[22] P. Sheng, B. Abeles, Phys. Rev. Lett. 28 (1972) 34.
[23] A.B. Kaiser, Rep. Prog. Phys. 64 (2001) 1.
[24] J.Y. Lee, K.T. Song, S.Y. Kim, Y.C. Kim, D.Y. Kim, C.Y. Kim, Synth. Met. 84 (1997) 137.
[25] A.N. Aleshin, K. Lee, J.Y. Lee, D.Y. Kim, C.Y. Kim, Synth. Met. 99 (1999) 27.
[26] C.O. Yoon, M. Teghu, D. Moses, A.J. Heeger, Y. Cao, T.-A. Chen, X. Wu, R.D. Rieke, Synth. Met. 75 (1995) 229.
[27] A.J. Epstein, W.-P. Lee, V.N. Prigodin, Synth. Met. 17 (2001) 9.
[28] A.B. Kaiser, Adv. Mater. 13 (2001) 927.
[29] L. Barton, Verres Refr. 20 (1966) 328.
[30] T. Nakajima, Conference on Electric Insulation and Dielectric Phenomena, National Academy of Sciences, Washington, DC, 1972, p. 168.
[31] H. Namikawa, J. Non-Cryst. Solids 18 (1975) 173.
[32] E. Singh, A.K. Narula, R.P. Tandon, A. Mansingh, S. Chandra, J. Appl. Phys. 80 (1996) 985.
[33] R. Singh, A.K. Narula, Synth. Met. 82 (1996) 245.